Ground Testing of the MISSE-16 Materials

Elena A. Plis*
Georgia Tech Research Institute (GTRI), Atlanta, GA, 30318, USA; Assurance Technology Corporation, Carlisle, MA, 01741, USA

Miles T. Bengtson†
National Research Council Research Associateship Program, 3550 Aberdeen Ave., Kirtland AFB, New Mexico 87117, USA

Daniel P. Engelhart‡
University of New Mexico, Albuquerque, NM, 87131, USA

Gregory P. Badura§
Georgia Tech Research Institute (GTRI), 925 Dalney St NW, Atlanta, GA 30318

Heather M. Cowardin¶
NASA Johnson Space Center, Orbital Debris Program Office, 2101 NASA Pkwy., Houston, TX 77058, USA

Jacqueline A. Reyes‖
University of Texas at El Paso, 500 W. University Ave., El Paso, TX, 79968, USA

Ryan C. Hoffmann, Alexey Sokolovskiy, Dale C. Ferguson**
Air Force Research Laboratory, Space Vehicles Directorate, USA, Kirtland AFB, Albuquerque, NM, 87117, USA

Jainisha R. Shah and Sydney Collman, ††
Assurance Technology Corporation, Carlisle, MA, 01741, USA

Timothy R. Scott‡‡
DuPont de Nemours, Inc, Durham, NC 27703, USA

External spacecraft materials play an important role in satellite protection from the harsh space environment. Research has shown that the physical, chemical, and optical properties of matter change continuously as a result of exposure to solar radiation and aggressive chemical species produced in Earth's upper atmosphere. Thorough knowledge of the material properties evolution throughout a planned mission lifetime helps to improve the reliability of spacecraft.

*Senior Research Engineer, Georgia Tech Research Institute (GTRI), 925 Dalney St NW, Atlanta, GA 30318; Assurance Technology Corporation, Carlisle, MA, 01741, USA

†Postdoctoral Fellow, National Research Council Research Associateship Program, 3550 Aberdeen Ave., Kirtland AFB, New Mexico 87117, USA

‡Research Professor, Department of Chemistry and Chemical Biology, University of New Mexico, 300 Terrace St NE, Albuquerque, NM, 87131.

§Research Scientist, Georgia Tech Research Institute (GTRI), 925 Dalney St NW, Atlanta, GA 30318.

¶Laboratory and In Situ Lead Orbital Debris Business Unit Manager, NASA Johnson Space Center, Orbital Debris Program Office, 2101 NASA Pkwy., Houston, TX 77058, USA

‖University of Texas at El Paso, 500 W. University Ave., El Paso, TX, 79968, USA

**Air Force Research Laboratory, Space Vehicles Directorate, USA, Kirtland AFB, Albuquerque, NM, 87117, USA

††Assurance Technology Corporation, Carlisle, MA, 01741, USA

‡‡Business Development Leader, Aerospace & Defense, DuPont de Nemours, Inc, Durham, NC 27703.

Moreover, the establishment of correlation factors between true space exposure and accelerated space weather experiments at ground facilities enables accurate prediction of on-orbit material performance based on laboratory-based testing. The presented work aims to evaluate the radiation effects of low Earth orbit (LEO) environment, namely, exposure to the high-energy electrons and atomic oxygen (AO), of heritage and novel spacecraft materials selection. The studied materials represent the "flight duplicates" of samples that are launched as a part of the 16th Materials International Space Station Experiment Flight Facility (MISSE-FF) mission in 2022.

I. Introduction

Exterior spacecraft materials play an important role in satellite protection from the strident space environment. Research has shown that the physical, chemical, and optical properties of matter change continuously as a result of exposure to solar radiation and aggressive chemical species produced in Earth's upper atmosphere [1–4]. Motivation of research reported here was the natural curiosity of team of scientists for fundamental understanding of the interactions between the harsh space environment and spacecraft materials. As humankind's forays into space become simultaneously more commonplace and ambitious, the need for this understanding becomes ever more important.Further, novel lightweight materials must be developed with improved long-term radiation shielding and mechanical properties for use in internal and external spacecraft systems. At low Earth orbit (LEO), the most destructive agents are atomic oxygen (AO) and unfiltered vacuum ultraviolet (VUV) radiation. Combined with charged particles (electrons) irradiation, AO and VUV may significantly degrade the outer spacecraft materials thus drastically reducing the lifespan of the spacecraft.

Up to date, the effect of LEO space weather exposure on durability and erosion of different materials was studied both in the laboratory space-simulated [5–9] and true space environment [10]. In particular, the interaction of LEO space weather, comprising AO/VUV- and some of high energy electron exposure, with a wide variety of spacecraft materials, including thermal control paints and organic polymers has been reported. However, in order to take advantage of the decades of materials research since the dawn of the space age, through vetting of novel materials is necessary and lacking.Independently, observation of spectral changes in materials exposed to the space environment including a "reddening" (i.e., decrease in optical reflectance with decreasing wavelength) of the spectra has been also reported, as well as potential schemes to utilize this feature for spacecraft material identification [e.g., [11]]. Still, no dynamic changes in material properties under exposure to the complex LEO environment were studied as well as utilization of these changes for remote spacecraft materials diagnosis.

Presented work reports on progress that our team made so far studying the effect of space-simulated low Earth orbital (LEO) environment on the optical, charge transport, and surface morphology properties of the selected spacecraft

polymers. Ground-based simulation of the space environment is experimentally challenging because the space environment varies wildly depending on orbit, solar conditions, and many other factors [12]. Simultaneous exposure of materials to the charge particles, VUV, and/or temperature may be hindered by different acceleration factors for particles and VUV flux, leading to significantly longer VUV irradiation times [13]. Oppositely, once a sequential exposure approach is utilized, materials are exposed to charging particles (protons, electrons), AO, and VUV, in successive steps. Thus, degradation induced by each environmental component may be monitored separately. In this work, we utilized space-simulated LEO environment comprised by, separately, high-energy electrons and AO exposure. Further, to correlate the evolution of material properties to those throughout a mission lifetime, we will employ the spectral reflectivity changes of the same materials induced by exposure to different components of the LEO environment during the six months long 16th Materials International Space Station Experiment Flight Facility (MISSE-FF) mission.

II. Experimental Details

A. Materials

The studied sample collection comprises several different class of polymers including polyimides (PIs), polyethylene terephthalates (PET) materials, liquid crystal polymers (LCP), PI/Polyhedral Oligomeric Silsesquioxanes (POSS) materials and carbon and glass reinforced polymers (CFRP and GFRP). Table 1 lists the materials and the material class that they belong to and fig. 1 demonstrates the visual appearance of materials in their pristine state.

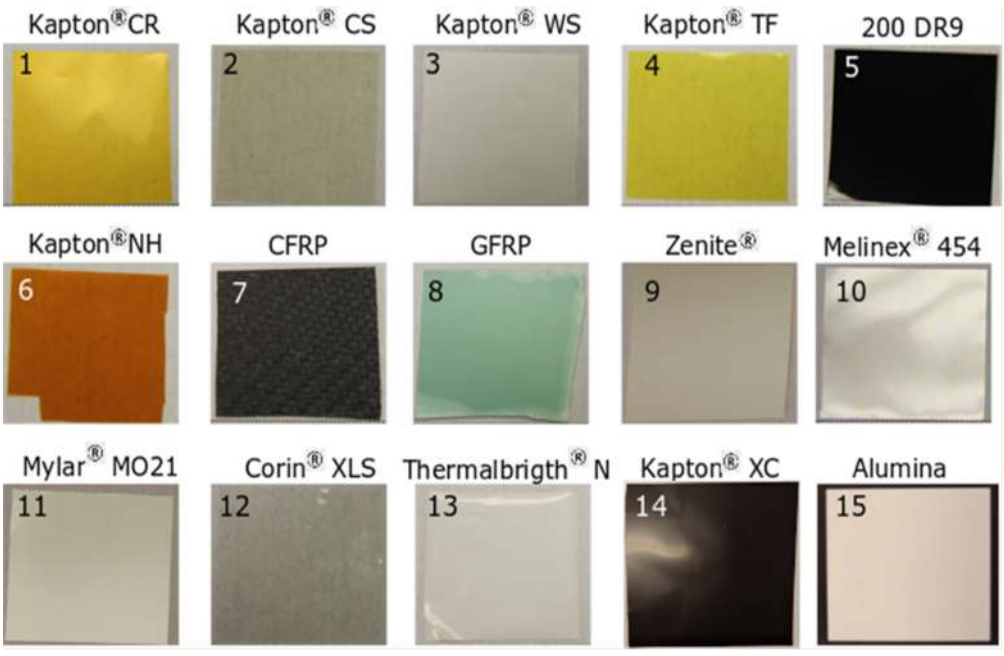

Fig. 1 The studied sample collection comprising several different classes of polymers as shown in Table 1

B. Irradiation Procedure

High energy electron and AO exposure were performed sequentially in the Jumbo space irradiation chamber at the SCICL [14] and at the Physical Sciences Inc. Materials were bombarded with high energy (100 keV) electrons produced by a mono-energetic Kimball Physics EG8105-UD electron flood gun. In according to [15], mean annual electron flux (>100 keV, electrons, orbit averaged) experienced by the ISS is $\sim 10^{13}$ electrons/cm^2/second. The maximum electron fluence the materials under investigation were exposed to is 8.5 x 10^{13} electrons/cm^2, which corresponds to approximately ten years at 600-800 km (LEO) orbit, delivered during 5.5 hours. Details of the electron irradiation procedure are reported elsewhere [16].

AO exposure was performed using the FAST source in according to ASTM-E2089-15. The effective peak atomic oxygen fluence during the exposure was 3.1 x 10^{20} O/cm^2 which corresponds to 6 weeks of LEO exposure. Details of AO-irradiation procedure may be found in [17].

C. Characterization Methods

Each material in its pristine and irradiates state was subjected to a characterization protocol schematically illustrated in fig. 2 using electron-irradiated Mylar®MO21 sample as an example. In particular, surface properties were accessed by the atomic force microscopy (AFM) and scanning electron microscopy (SEM) techniques, optical properties were characterized using the Hemispherical Conical Reflectance Factor (HCRF), the laboratory approximation of true Bidirectional Reflectance Distribution Function (BRDF) measurements, UV/Vis transmission and reflectance measurements, the directional hemispherical reflectance (DHR) measurements, and Fourier-Transform Infrared (FTIR) spectroscopic measurements. Further, effect of space-simulated exposure on charge transport properties was evaluated with direct current ASTM D-257 and the surface potential decay (SPD)[18] methods. In addition, mass loss of AO-exposed materials was estimated. This work will focus on space-weather induced changes of surface morphology and optical behavior of all studied materials measured by DHR (for electron-irradiated materials) and UV/Vis spectroscopy (for AO-exposed materials).

Surface morphology and roughness of studied materials was examined using Bruker Dimension ICON AFM allowing measurement of surface roughness up to 5 μm on areas as large as 200 μm x 200 μm. The DHR measurements of pristine and electron-irradiated samples were performed prior and during the electron irradiation procedure in according to the optical data acquisition procedure reported elsewhere [19]. Transmission measurements of AO-exposed materials were performed with the Gary 5000 UV-Vis-NIR spectrometer.

D. Results and Discussion

Average surface roughness (R_a) values of pristine, irradiated with high energy electrons, and AO-exposed materials are summarized in Table 1. R_a values are average of several 5μm x 5μm scans taken at different parts of the sample.

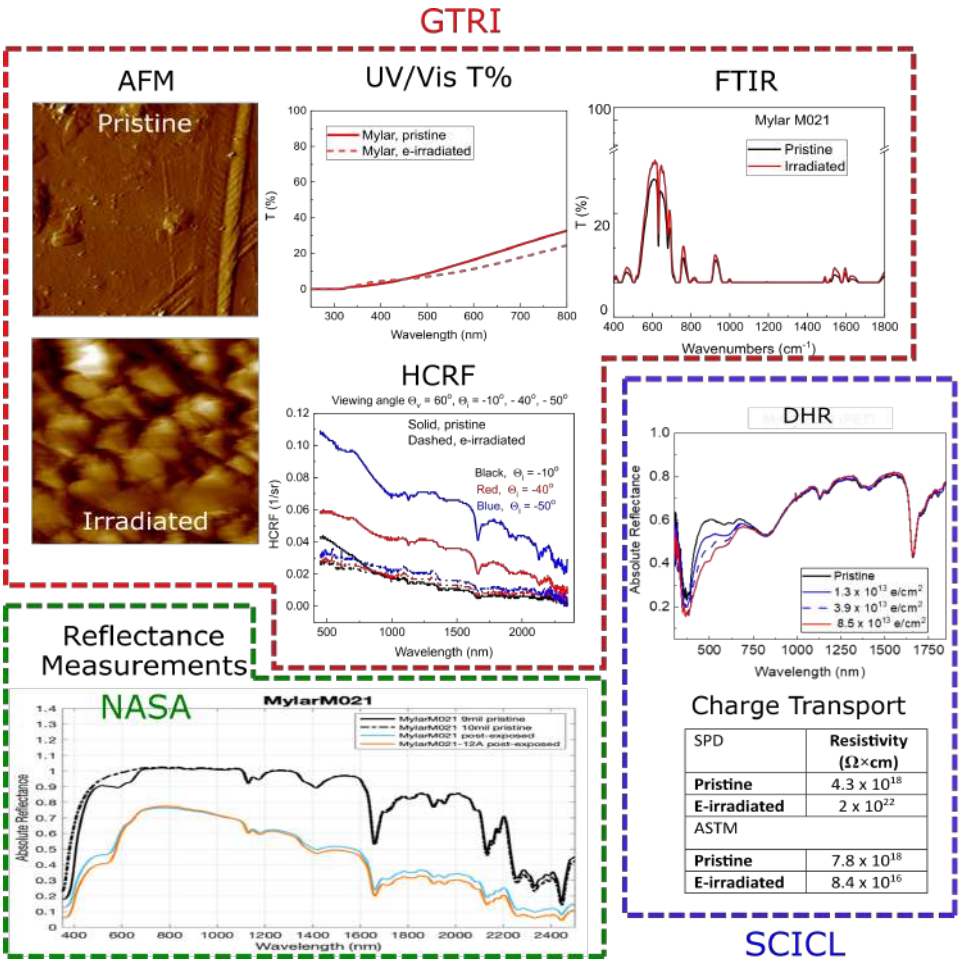

SPD	Resistivity (Ω×cm)
Pristine	4.3 x 10^{18}
E-irradiated	2 x 10^{22}
ASTM	
Pristine	7.8 x 10^{18}
E-irradiated	8.4 x 10^{16}

Fig. 2 Illustration of material properties characterization protocol utilized for pristine and irradiated materials using electron-irradiated Mylar®MO21 sample as an example. Here GTRI and SCICL stand for the Georgia Tech Research Institute and the Spacecraft Charging and Instrument Calibration Laboratory, respectively.

Note, that roughness of CFRP material was too large even in its pristine form to be measured reliably with the AFM technique.

Most of the electron-irradiated materials from the Kapton®family demonstrated significant reduction of R_a roughness (HN, CS, WS, XC, DR9) after electron irradiation. Kapton®CR did not change, and only one PI material (Kapton®TF) showed surface roughening after electron bombardment. Surface roughness of PET materials also reduced after irradiation. Surface of LCP (Zenite®), similar to Kapton®TF, revealed the increased R_a after irradiation. Both POSS materials became smoother after electron exposure, however, CORIN®XLS demonstrated a factor of 4.3 roughness reduction whereas surface roughness of Thermalbright®N changed slightly. Finally, the GFRP material was factor of 3 smoother after electron irradiation.

Exposure of polymer materials to AO at 8 km/s is sufficient to break the polymer bonds and induce oxidative decomposition, resulting in substantial erosion of polymer surfaces which manifests itself as the mass loss, thinning,

Table 1 R_a roughness values of pristine, irradiated with high energy electrons, and AO-exposed materials.

No.	Trade name	Abbrev.	R_a (nm) Pristine	R_a (nm) E-irradiated	R_a (nm) AO-exposed
1	Kapton ®CR	PI	26.7	25.6	62.9
2	Kapton ®CS	PI	5.5	2.0	15.4
3	Kapton ®WS	PI	72.3	32.4	20.1
4	Kapton ®TF	PI	5.5	12.3	136.3
5	200DR9®	PI	26.7	4.6	111.0
6	Kapton®HN	PI	11.4	2.5	91.0
7	Economyplate™	CFRP	N/A	N/A	N/A
8	G-10/FR4 Glass Epoxy	GFRP	12.2	4.6	218.0
9	Zenite®	LCP	14.9	25.1	71.9
10	Melinex®454	PET	8.2	5.0	116.7
11	Mylar®MO21	PET	7.8	3.6	187.2
12	CORIN®XLS	POSS	9.4	2.2	14.3
13	Thermalbright®N	POSS	52.5	47.7	74.6
14	Kapton®XC	PI	56.2	34.5	161.0

and texture roughening. AO exposure clearly affected the surface roughness of the studied materials. All polymers from Kapton®family, excluding Kapton, revealed a matter surface which is result of O-atom erosion leading to the microscopic roughness of these samples. Post-exposed Kapton®WS retained the pristine-like visual appearance with reduced R_a roughness compared to its pristine state. Both PET samples (Mylar®M021 and Melinex®454) were severely degraded after AO-exposure, with R_a roughness increasing by more than factor of ten as a result of AO-erosion. AO-induced damage of LCP, GFRP, and CFRP materials was also easily observed. The AO-exposed surfaces of these samples became less glossy. Finally, R_a roughness of two POSS materials, CORIN®XLS and Thermalbright®N, increased insignificantly suggesting good resistance of these materials to AO-induced erosion.

Results of in-situ DHR measurements on transparent and opaque materials are summarized in 3. All measured materials demonstrated the reflectance changes with electron exposure. Interesting that degradation of both studied POSS materials was minimal suggesting good resistance of the POSS films for electron bombardment. In fig. 4 the observed DHR data trends are summarized for every material in more visual form. In shorter wavelength region, materials apart from POSS, revealed the reduction of signal. Both POSS materials, as mentioned earlier, did not change considerably. Generally no signal degradation was observed beyond twelve hundred nanometers. Interesting, that one of PET materials, Mylar®M021, became more reflective in the longer wavelength range.

Results of UV-Vis transmission measurements of of pristine and AO-exposed transparent and opaque materials from the studied material selection are presented in Fig. 5.

Light transmission characteristics of all studied materials considerably degraded after AO exposure. The measurable (e.i., transparent enough) materials from the Kapton®family (HN, TF, CR, and CS), demonstrated reduction of transmission. Kapton®WS, Thermalbrigh®N, GFRP, and Zenite®materials have low light transmittance in their pristine

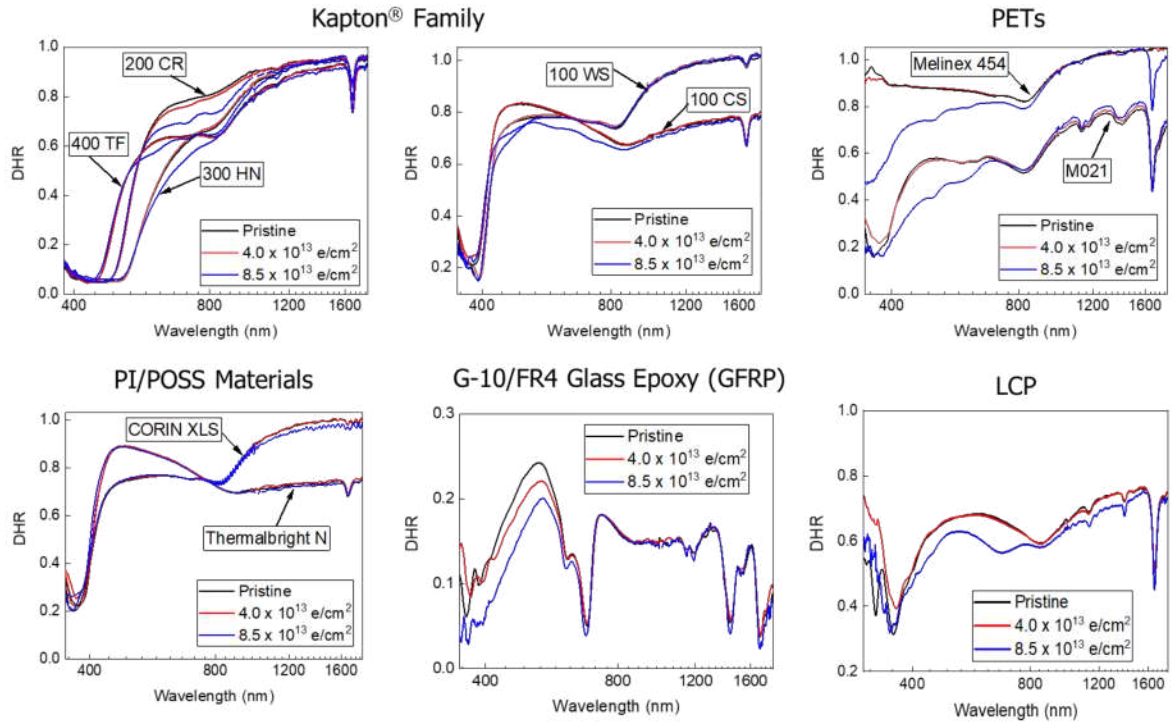

Fig. 3 The DHR measurements of transparent and opaque materials from the studied material selection irradiated with high energy electrons.

Material	Trade name	Wavelength region (nm)		
		400 - 800	800 - 1200	1200 - 1600
Kapton®	CR			
	TF			
	HN			
	CS			
	WS			
PET	Mylar® M021			
	Melinex® 454			
PI/POSS	CORIN® XLS			
	Thermalbright® N			
LCP	Zenite®			
GFRP	G-10/FR4 Glass Epoxy			

Signal decreases No change Signal increases

Fig. 4 The observed DHR data trends of electron-irradiated transparent and opaque materials from the studied material selection.

state (0.1-0.2 %), and after AO exposure their appearance has changed to completely opaque. Transmission of both PET samples degraded after AO exposure considerably. CORIN®XLS, as expected, was not affected be the AO-exposure. The transmission curve of this material did not show significant changes in 400 – 2000 nm wavelength region. However, transmission of AO-exposed material increased around 300 nm. It should be noted that all measured curves possess a

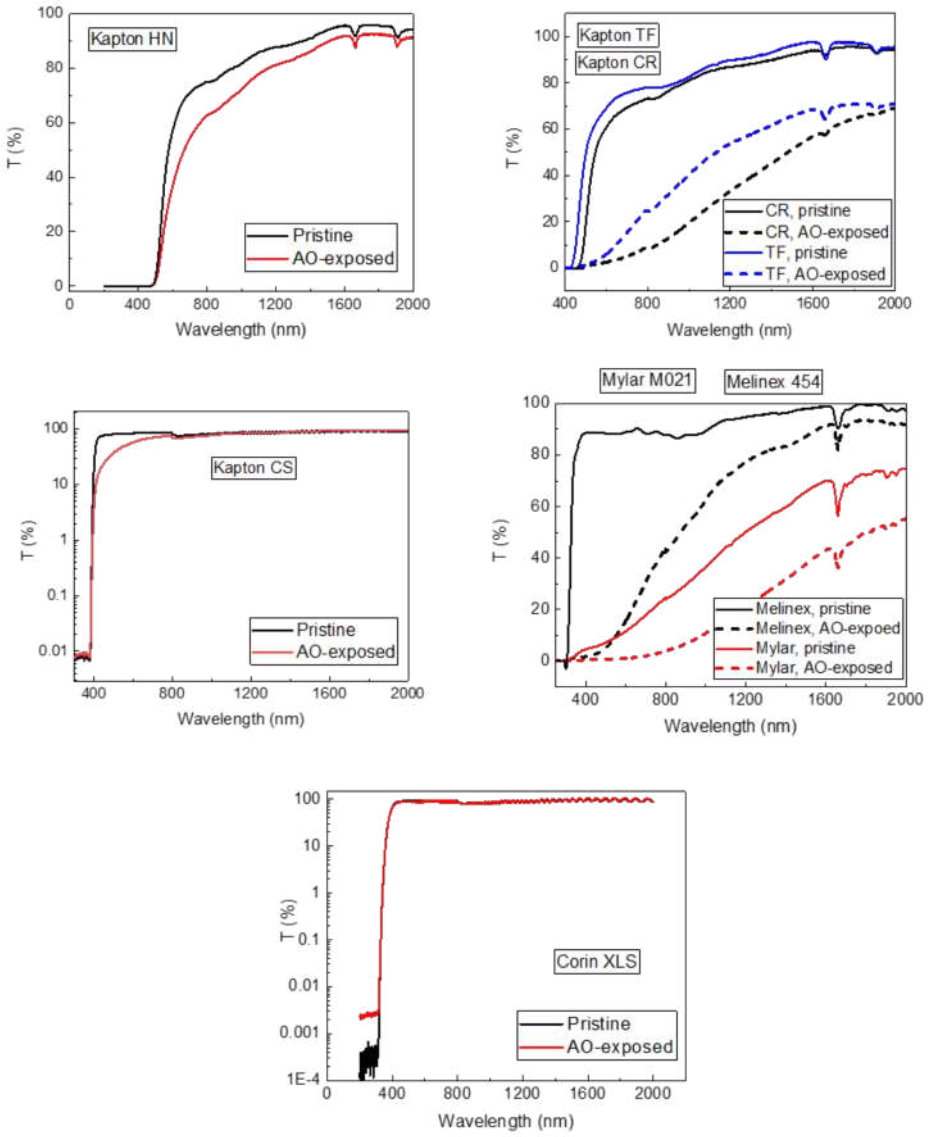

Fig. 5 UV-Vis transmission measurements of pristine and AO-exposed transparent and opaque materials from the studied material selection.

kink at 800 nm which is an instrumental artefact corresponding to the change of detectors in Gary 5000 during the measurements.

E. MISSE-FF Materials Integration

The identical material set will be installed on each face of MISSE-FF to learn about separate effects of LEO environmental components on these spacecraft materials, in particular, Ram (direction of travel) with dominant AO exposure, Zenith (direction away from Earth), with dominant VUV exposure, and Wake (opposite to the travel direction), with high energy electrons exposure. To closely monitor the optical changes of materials during the mission, we

proposed to upgrade the MISSE-FF with different illumination scheme, including White and IR LED illumination sources, and high resolution camera which will record RGB and IR color data. This upgraded hardware will stay onboard of MISSE-FF available for future scientific work.

MISSE-16 flight duration will be approximately six-months; daily image of each sample will be taken for the first 30 days; weekly image of each sample for the next two months; monthly images for the remaining duration of the mission. Thus, we will monitor the aging of the materials, which will manifest itself as a reflectivity change, almost in real time during the initial stage of the LEO exposure, and then very closely during the rest of the mission.

MISSE-FF materials integration along with camera board integration for the MISSE-16 mission were performed on September 2021. Identical MISSE-FF carriers were prepared for Ram, Zenith, and Wake faces of MISSE-FF. Many of our materials were mounted in multiple layers, to get the average thickness of 10 mils. Fig. 6 shows the camera board assembly and the sample image delivered by the Basler daA1600 camera.

Fig. 6 (left) MISSE-FF camera board assembly and (right) sample image delivered by the Basler daA1600 camera. Image credit: AFRL.

III. Conclusion

Thorough characterization of material properties of different spacecraft materials during the simulated space weather experiments is important for establishment of correlation factors between true space-exposure and accelerated space weather conditions at ground facilities as well as enabling accurate prediction of on-orbit material performance based on laboratory-based testing. This work focuses on characterization of surface morphology and optical properties of selected spacecraft materials under independent LEO-simulated electron irradiation and AO exposure.

Funding Sources

This work was partially supported by Air Force Office of Scientific Research, Remote Sensing and Imaging Physics Portfolio (Dr. Michael Yakes) Grant 20RVCOR024 and Georgia Tech Research Institute Independent Research and Development (IRAD) program.

Acknowledgments

Authors gratefully acknowledge Physical Sciences, Inc., especially Drs. Daniel M. Hewett and David B. Oakes, for conducting AO-exposure experiments. Authors also would like to thank DuPont de Nemours, Inc, for providing polyimide materials for this research.

Disclaimers

The views expressed are those of the author and do not necessarily reflect the official policy or position of the Department of the Air Force, the Department of Defense, or the U.S. government.Statement from DoD: The appearance of external hyperlinks does not constitute endorsement by the United States Department of Defense (DoD) of the linked websites, or the information, products, or services contained therein. The DoD does not exercise any editorial, security, or other control over the information you may find at these locations.

Trade names and trademarks are used in this report for identification only. Their usage does not constitute an official endorsement, either expressed or implied, by the National Aeronautics and Space Administration.

Approved for public release; distribution is unlimited. Public Affairs release approval number ....

References

[1] Dooling, D., *Material selection guidelines to limit atomic oxygen effects on spacecraft surfaces*, Marshall Space Flight Center, 1999.

[2] de Groh, K. K., and Banks, B. A., "MISSE 2 PEACE polymers erosion morphology studies," *Proceedings of the International Symposium on Materials in a Space Environment (ISMSE-11)*, 2009.

[3] Miller, S. K., and Dever, J. A., "Materials international space station experiment 5 polymer film thermal control experiment," *Journal of Spacecraft and Rockets*, Vol. 48, No. 2, 2011, pp. 240–245.

[4] Ouchen, F., Aga, R., Harvey, M., and Heckman, E., "Space survivability for printed electronics applications," *Flexible and Printed Electronics*, Vol. 6, No. 1, 2021, p. 015012.

[5] Tagawa, M., and Yokota, K., "Atomic oxygen-induced polymer degradation phenomena in simulated LEO space environments: How do polymers react in a complicated space environment?" *Acta Astronautica*, Vol. 62, No. 2-3, 2008, pp. 203–211.

[6] Awaja, F., Moon, J. B., Zhang, S., Gilbert, M., Kim, C. G., and Pigram, P. J., "Surface molecular degradation of 3D glass polymer composite under low earth orbit simulated space environment," *Polymer Degradation and Stability*, Vol. 95, No. 6, 2010, pp. 987–996.

[7] Jin, S., Son, G., Kim, Y., and Kim, C.-G., "Enhanced durability of silanized multi-walled carbon nanotube/epoxy nanocomposites under simulated low earth orbit space environment," *Composites Science and Technology*, Vol. 87, 2013, pp. 224–231.

[8] Tonon, C., Duvignacq, C., Teyssedre, G., and Dinguirard, M., "Degradation of the optical properties of ZnO-based thermal control coatings in simulated space environment," *Journal of Physics D: Applied Physics*, Vol. 34, No. 1, 2001, p. 124.

[9] Dworak, D. P., Banks, B. A., Karniotis, C. A., and Soucek, M. D., "Evaluation of protective silicone/siloxane coatings in simulated low-earth-orbit environment," *Journal of Spacecraft and Rockets*, Vol. 43, No. 2, 2006, pp. 393–401.

[10] Dever, J., Banks, B., de Groh, K., and Miller, S., "Degradation of Spacecraft Materials in Handbook of Environmental Degradation of Spacecraft Materials, Kutz, M. Editor," , 2005.

[11] Abercromby, K., Okada, J., Guyote, M., Hamada, K., and Barker, E., "Comparisons of ground truth and remote spectral measurements of the formosat and ande spacecraft," *Proceedings of the 2006 AMOS Technical Conference*, Citeseer, 2006.

[12] Gordo, P., Frederico, T., Melício, R., Duzellier, S., and Amorim, A., "System for space materials evaluation in LEO environment," *Advances in Space Research*, Vol. 66, No. 2, 2020, pp. 307–320.

[13] Duzellier, S., Gordo, P., Melicio, R., Valério, D., Millinger, M., and Amorim, A., "Space debris generation in GEO: Space materials testing and evaluation," *Acta Astronautica*, Vol. 192, 2022, pp. 258–275.

[14] Cooper, R., and Hoffman, R., "Jumbo space environment simulation and spacecraft charging chamber characterization," Tech. rep., Air Force Research Laboratory, Space Vehicles Directorate Kirtland AFB . . . , 2015.

[15] Plis, E. A., Engelhart, D. P., Cooper, R., Johnston, W. R., Ferguson, D., and Hoffmann, R., "Review of radiation-induced effects in polyimide," *Applied Sciences*, Vol. 9, No. 10, 2019, p. 1999.

[16] Engelhart, D. P., Plis, E., Humagain, S., Greenbaum, S., Ferguson, D., Cooper, R., and Hoffmann, R., "Chemical and electrical dynamics of polyimide film damaged by electron radiation," *IEEE Transactions on Plasma Science*, Vol. 45, No. 9, 2017, pp. 2573–2577.

[17] Plis, E., Bengtson, M., Engelhart, D. P., Badura, G., Scott, T., Cowardin, H., Reyes, J., Hoffmann, R., Sokolovskiy, A., Ferguson, D. C., et al., "Characterization of novel spacecraft materials under high energy electron and atomic oxygen exposure," *AIAA SCITECH 2022 Forum*, 2022, p. 0797.

[18] Frederickson, A. R., and Dennison, J., "Measurement of conductivity and charge storage in insulators related to spacecraft charging," *IEEE Transactions on Nuclear Science*, Vol. 50, No. 6, 2003, pp. 2284–2291.

[19] Bengtson, M., Maxwell, J., Hoffmann, R., Cooper, R., Schieffer, S., Ferguson, D., Johnston, W. R., Cowardin, H., Plis, E., and Engelhart, D., "Optical characterization of commonly used thermal control paints in a simulated GEO environment," *The Advanced Maui Optical and Space Surveillance Technologies Conference*, 2018, p. 33.